



This is a repository copy of *Longitudinal MRI brain studies in live adult zebrafish*.

White Rose Research Online URL for this paper:

<https://eprints.whiterose.ac.uk/195547/>

Version: Published Version

---

**Article:**

Hamilton, N. [orcid.org/0000-0002-3299-9133](https://orcid.org/0000-0002-3299-9133), Allen, C. and Reynolds, S. [orcid.org/0000-0002-6463-8471](https://orcid.org/0000-0002-6463-8471) (2023) Longitudinal MRI brain studies in live adult zebrafish. *NMR in Biomedicine*, 36 (7). e4891. ISSN 0952-3480

<https://doi.org/10.1002/nbm.4891>

---

**Reuse**

Items deposited in White Rose Research Online are protected by copyright, with all rights reserved unless indicated otherwise. They may be downloaded and/or printed for private study, or other acts as permitted by national copyright laws. The publisher or other rights holders may allow further reproduction and re-use of the full text version. This is indicated by the licence information on the White Rose Research Online record for the item.

**Takedown**

If you consider content in White Rose Research Online to be in breach of UK law, please notify us by emailing [eprints@whiterose.ac.uk](mailto:eprints@whiterose.ac.uk) including the URL of the record and the reason for the withdrawal request.



[eprints@whiterose.ac.uk](mailto:eprints@whiterose.ac.uk)  
<https://eprints.whiterose.ac.uk/>

## RESEARCH ARTICLE

# Longitudinal MRI brain studies in live adult zebrafish

Noémie Hamilton<sup>1,2,3</sup>  | Claire Allen<sup>1</sup> | Steven Reynolds<sup>3</sup> 

<sup>1</sup>The Bateson Centre, University of Sheffield, Sheffield, UK

<sup>2</sup>Neuroscience Institute, University of Sheffield, Sheffield, UK

<sup>3</sup>Department of Infection, Immunity and Cardiovascular Disease, University of Sheffield, Sheffield, UK

## Correspondence

Noémie Hamilton and Steven Reynolds, Department of Infection, Immunity and Cardiovascular Disease, University of Sheffield, Sheffield S10 2TN, UK. Email: [n.m.hamilton@sheffield.ac.uk](mailto:n.m.hamilton@sheffield.ac.uk) and [steven.reynolds@sheffield.ac.uk](mailto:steven.reynolds@sheffield.ac.uk)

## Funding information

University of Sheffield; University of Sheffield Alumni Fund; Association Européenne contre les Leucodystrophies, Grant/Award Number: ELA2016-012F4

## Abstract

Zebrafish (*Danio rerio*) has been successfully used for decades in developmental studies and disease modelling. The remarkable uptake of zebrafish as a model system is partly due to its transparency during the early weeks of its development, allowing in vivo imaging of cellular and molecular processes. However, this key advantage wears off when tissues become opaque as the animal reaches juvenile and adult stages, rendering access to tissues for live imaging and longitudinal studies difficult. Here we provide a novel approach to image and assess tissue integrity of adult zebrafish using MRI on live zebrafish suitable for longitudinal studies. We built a 3D-printed life support chamber and designed a protocol-directed sedation regime to recover adult zebrafish after scanning in a 9.4 T MRI scanner. Our life support chamber is cheap and easy to create using 3D printing, allowing other groups to copy our template for quick setup. Additionally, we optimized the delivery of contrast agent to enhance brain signals in order to refine current delivery, usually delivered intravenously in rodents. We show here that immersion in gadolinium was a viable alternative to intraperitoneal injection to reduce  $T_1$  relaxation times. This resulted in protocol refinement as per the 3Rs guidelines and improved image contrast in adult zebrafish disease models. In conclusion, we provide here a detailed methodology to allow longitudinal studies of brain tissue integrity of adult zebrafish, combining safe and efficient delivery of contrast agent and live MRI. This technique can be used to bridge the gap between in vivo studies and longitudinal brain analysis in adult zebrafish, and can be applied to the ever-growing number of adult zebrafish models of ageing and neurodegenerative diseases.

## KEYWORDS

brain MRI, gadolinium contrast agent, live adult zebrafish, longitudinal studies

**Abbreviations:** 3Rs, replace, reduce, refine; FOV, field of view; GCA, gadolinium-based contrast agent; I.D., internal diameter; IP, intra-peritoneal; IQR, interquartile range; MS-222, tricaine methanesulfonate; MSME, multi-slice multi-echo; NEX, number of excitations; PBS, phosphate buffered saline; PFA, paraformaldehyde; PLA, polylactic acid; RARE/RARE-VTR, rapid acquisition with refocused echoes/variable repetition time; ROI, region of interest; SEM, standard error of mean; SNR, signal to noise ratio.

Noémie Hamilton and Steven Reynolds contributed equally.

This is an open access article under the terms of the [Creative Commons Attribution](https://creativecommons.org/licenses/by/4.0/) License, which permits use, distribution and reproduction in any medium, provided the original work is properly cited.

© 2022 The Authors. *NMR in Biomedicine* published by John Wiley & Sons Ltd.

## 1 | INTRODUCTION

Neurodegenerative diseases are devastating and affect millions of people in the UK. Animal models are essential to characterize and understand brain tissue morphology, integrity and function. In accordance with the refinement principle of the 3Rs (replace, reduce, refine), neurodegenerative research has steadily transitioned from rodent to zebrafish models, which are a lower neurophysiological, versatile and cost-effective species. Zebrafish are a popular research model for studying neurological diseases, such as Parkinson's, multiple sclerosis, leukodystrophies and epilepsy.<sup>1–6</sup> Most of the work into these neurological conditions is conducted on transparent juvenile fish, which are amenable to real-time optical imaging techniques. However, longitudinal monitoring of disease progression is visually limited by the opacity of adult zebrafish restricting the scope of data collection at these later stages.

MRI is a well known non-invasive medical tool for diagnosing patients suffering from neurodegenerative diseases and is ideally suited for longitudinal studies. It can image both tissue integrity and function throughout the brain, with rodent models underpinning much of this work.<sup>7,8</sup> Pre-clinical MRI has previously been used to study human disease models in zebrafish, where the application of ultrahigh field (>7 T), powerful gradient systems and bespoke small volume coils permits relatively high-resolution images—of the order of 10  $\mu\text{m}$  or greater. Most of these have used fixed tissue<sup>9,10</sup>; however, more recently publications reported MRI scanning of live fish.<sup>11–13</sup> Life support for the fish has required the implementation of an MRI compatible flow tank, which can produce turbulence leading to a degradation in imaging quality. Furthermore, a wider field of view (FOV) is required that encompasses the flow chamber to prevent wrap-around effects and necessitates more phase encoding steps, i.e., longer acquisition times, for a given resolution.

In our study, we have developed a prototype life support chamber for zebrafish that removes the need for a water filled flow chamber. The chamber can be used in a vertical bore MRI scanner with anaesthesia supplied by readily available laboratory equipment, i.e., syringe pumps. Supplying of anaesthesia by intubation directly to the fish mouth removes the need for water to surround the gills, therefore reducing turbulence, as the water drains down the flanks of the fish keeping it moist and minimizes fish movement. Additionally, the FOV in the phase encoding direction can be reduced by placing it along the sagittal axis of the fish. Cost and ease of fabrication were prioritized during the design of the chamber: consideration was given to availability of parts and materials. The chamber is 3D printable, which is cheap and rapid, allowing the chamber either to be reused or to be a single-use item if, for instance, spread of infection was a concern. The live chamber permitted scanning of anaesthetized adult zebrafish for 2 h, followed by full recovery.

Gadolinium-based contrast agents (GCAs) are commonly used as a method to increase tissue contrast and/or reduce imaging time.<sup>14</sup> These agents have also been applied to zebrafish MRI for live imaging in the heart<sup>12</sup> and fixed or freshly sacrificed fish brain tissue.<sup>10</sup> Whilst intraperitoneal (IP) injection is a commonly accepted administration route for small animals it can lead to tissue injury or mis-dosing due to small volumes of injected fluid. In this study, we allowed fish to swim freely immersed in GCA mixed with fish water to examine its effect on  $T_1$  and  $T_2$  values and compared this with IP injected animals. Our study has developed a novel chamber to safely hold a zebrafish for MRI and refined current contrast agent administration protocol to comply with the 3Rs approach.

## 2 | MATERIALS AND METHODS

### 2.1 | Zebrafish husbandry and ethics

All zebrafish were raised in the Biological Services Aquarium at the University of Sheffield in the UK Home Office-approved aquarium and maintained following standard protocols.<sup>15</sup> Tanks were maintained at 28 °C with a continuous recirculating water supply and a daily light/dark cycle of 14/10 h. All procedures were performed on adult zebrafish to standards set under AWERB (animal welfare and ethical review body) and UK Home Office-approved protocols (Project Licence P254848FD). Fish were transported to the MRI facility in a polystyrene carrier box containing a single tank. Fish were kept in the box to maintain a constant temperature in a designated animal room until needed for experiment on the same day. The MRI facility suite is kept air conditioned at 21 °C and no heating was provided to the fish whilst they were in the scanner.

### 2.2 | Zebrafish life support chamber

The fish life support chamber was intended to supply water directly to the animal without the exterior water surrounding the fish. It was designed to be inserted into a 10 mm MRI volume coil and provide easy access for fish loading and observation. The chamber was modelled in open-source software Blender ([www.blender.org](http://www.blender.org)) and 3D printed using Cura software and an Ultimaker 2+ Extended 3D printer (both Ultimaker, Utrecht, The Netherlands). Objects were printed with polylactic acid (PLA); see Figure 1. The PLA main body (1 in Figure 1) supports all components and collects water for drainage through the bottom (2). The zebrafish was supported (3) by four flexible transparent acrylic rods (1 mm diameter, ~5 cm in length; 4D Modelshop Ltd, London, UK) that slot into the main body and a PLA retaining plate (4) at the top. Water was supplied to the fish via

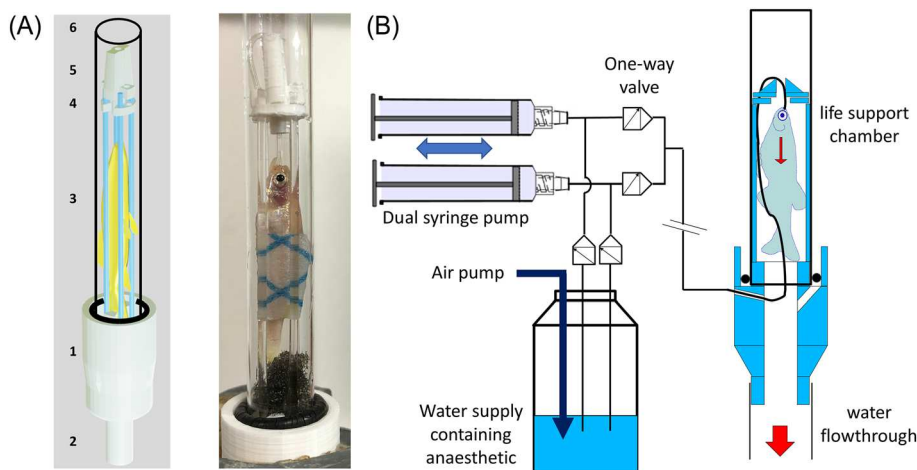


**FIGURE 1** 3D-printed chamber supports zebrafish adults during MRI scans. (A), The fish life support chamber was composed of the following. (1) A 3D-printed main body that supports the remaining components. It comprises a central large hole for water for drainage at the bottom (2) and smaller side hole, angled downwards, for the anaesthetic water supply tube. Four flexible fish support rods (3) are inserted into the main body and are held at the top by a retaining plate (4). Water supply was provided by a tube that enters via a side hole in the main body and passes into the fish's mouth via a 3D-printed plastic tube guide (5) that fits to the retaining plate (4) at the top. Water tightness was achieved using a 10 mm glass NMR tube (6) that fits over the upper part of the assembly and is sealed to the main body (1) with O-rings. (B), A constant flow water supply system was provided to the fish using two syringe pumps. Oxygenated water was drawn from a main reservoir that contained anaesthetic. The pumps worked in push/pull tandem so that one is filling as the other supplies water to the fish. See the main text for details.

a polyvinyl chloride tube (not shown on the 3D model) that passed into the side of the main body, up past the fish, through a PLA guide (5) and into the fish's mouth. The compartment was made watertight using a 10 mm glass NMR tube (6) that fitted over the upper part of the assembly and was sealed to the main body (1) with an O-ring. To maintain the fish physiology, oxygenated water (containing anaesthetic, see below) passed into the fish's mouth, out via the gills and down its flanks. Water was drained through a long tube to the bottom of the probe and into a collecting jar. To allow for adjustment of the water supply tube it was not sealed to the main body but relied on the design of the chamber, i.e., the inlet hole sloped downwards into the chamber, so it could be adjusted for the fish, whilst preventing water egress through its access hole. Models for 3D printing parts are publicly available here: <https://figshare.com/s/c9d1df9808540583450e>.

### 2.3 | Zebrafish water supply

The tube inserted into the fish's mouth consisted of a short, ~20 cm, 0.25 mm internal diameter (I.D.) tube that was extended with a 0.89 mm I.D. tube approximately 2 m in length (S3 and S54-HL Tygon respectively, Cole-Parmer, St Neots, UK). Continuous water supply was maintained by two Aladdin NE-1000 syringe pumps (World Precision Instruments, Hitchin, UK) that were synchronized to draw oxygenated water from a main reservoir that contains anaesthetic. The pumps were programmed to work in tandem such that one filled as the other supplied water to the fish at 3 mL/min. 10 mL syringes were used so that each one cycles over about 5 min (fill/discharge) (Figure 1B). Oxygenated water also contained sedative; see below.

### 2.4 | Zebrafish anaesthesia, scanning and recovery

We designed a dual anaesthetic regime using both tricaine methanesulfonate (MS-222, Sigma—Catalogue No E10521, Gillingham, UK) and benzocaine (Sigma, E1501) to fine-tune the depth of anaesthesia during the entire process. Tricaine at 160 mg/mL was used to initially sedate the fish and keep it immobilized while handling. Tricaine stock was made at 4 g/L in filtered system water, with pH adjusted to 7.4 using 1 M Tris. A brown glass bottle protected the stock solution from light and was stored in the fridge. Subsequent tricaine solutions were made using tricaine stock and E3 water (a medium fortified with extra calcium and salt to maintain zebrafish.  $10\times$  E3: 5 mM NaCl, 0.17 mM KCl, 0.33 mM  $\text{CaCl}_2$ , 0.33 mM  $\text{MgSO}_4$ ), diluted to  $1\times$  E3 with distilled water.<sup>15,16</sup> The anaesthetic solution concentrations were made with high accuracy: 160 mg/mL tricaine (4 mL in 96 mL of E3) and 120 mg/mL tricaine (3 mL in 96 mL of E3). Benzocaine stock was made at 50 mg/mL by dissolving in 70% ethanol. This was aliquoted into 750  $\mu\text{L}$  and stored at  $-20^\circ\text{C}$  until usage. Benzocaine was used at the final concentration of 35 mg/L (using 700  $\mu\text{L}$  in 1 L to directly feed the syringe pumps).

For initial anaesthesia, fish were transferred using a net to a beaker containing 100 mL of 160 mg/mL tricaine. When the fish stopped moving and responding to touch, it was lifted out of the beaker and transferred to a shallow bath of 160 mg/mL tricaine in a clean petri dish. There, the fish was wrapped in a thin rectangle of multipurpose cloth (Spontex code/SKU: 19900074), which allowed the fish to be gently held vertically without slipping or damaging its scales. This process took about 3 min. Fish were vertically inserted between the pliable rods of the live chamber (see above), ensuring that the feeding tube was positioned ventrally to stop any water artefacts appearing in the image. During the positioning process, the fish was kept moist by dripping 160 mg/mL tricaine on its head. Once intubated, the tricaine concentration was reduced to 120 mg/mL while the fish and cloth were secured by a glass tube covering the chamber. The intubated fish was kept hydrated during image acquisition by water expelled from the fish's gills that was caught by a soft cloth wrapped around its body and a sponge placed under the tail (Figure 2). The whole chamber was then inserted inside the MRI probe, securely taped to avoid slippage and inserted into the 9.4 T MRI scanner. Flowing intubating liquid was then switched from 120 mg/mL tricaine to 35 mg/l of Benzocaine to ensure long-term safe sedation. The loading process took only a few minutes and scanning time was limited to less than 2 hours. A step-by-step protocol is provided as a supplemental file. During this project (including chamber development), we scanned a total of 29 fish across a range of ages (median 17 months, range 10–18 months).

After scanning, fish were carefully taken out of the chamber and deposited in a tank of fresh E3 water at 23 °C. Using a lower than usual temperature allowed the animal to adjust after being held in the scanner at about 21 °C. After scanning, fish recovery was recorded as free-swimming behaviour for at least 30 min, after which animals were culled using an overdose of tricaine and fixed in 4% paraformaldehyde (PFA) using the immersion–fixation regulated killing procedure. Some recovered animals were kept for several hours and showed normal behaviour throughout this period.

## 2.5 | Gadolinium administration

Gadolinium MRI contrast agent (Gadovist → 1.0 mmol/mL stock—Bayer Radiology, Leverkusen, Germany) was administered using two different routes.

1. For immersion, fish were left free swimming in a bath of 100 mL E3 water containing 60 mmol/L of Gadovist (6.6 mL Gadovist in 100 mL of E3 water) for at least 2 h.
2. For IP injection, fish were anaesthetized using tricaine at 160 mg/mL until the fish stopped moving and responding to touch. The fish was transferred to a soft sponge, laid in a petri dish and saturated with tricaine water at 160 mg/mL, with a cut deep enough to accept the fish on its back. Using an insulin syringe (BD Micro-Fine+ Demi U-100 Insulin 0.3 mm 30G × 8 mm, Fisher Scientific, Loughborough, UK), 5 µL of 1:2 Gadovist stock diluted in phosphate buffered saline (PBS) (0.5 mmol/mL) was injected into the peritoneal cavity of the fish. The fish was then kept in 160 mg/mL tricaine to wrap in the cloth and placed in the chamber.
3. Control fish were either injected with PBS, as for (2) above, or swimming in E3 water.

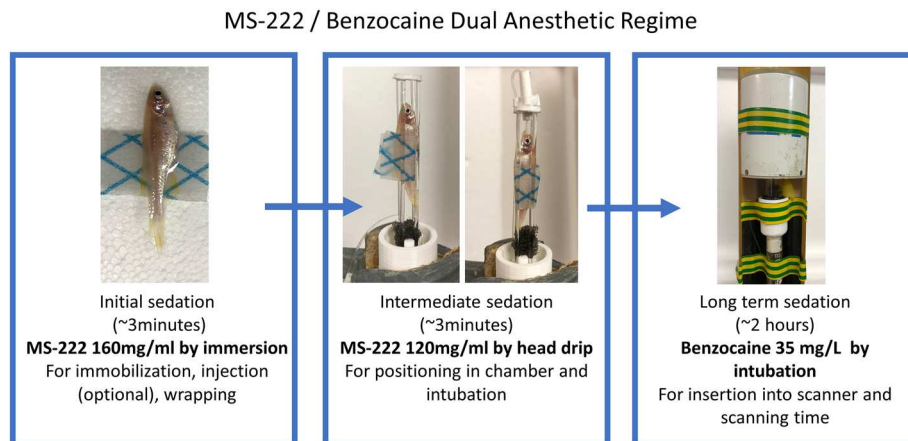


**FIGURE 2** Animal positioning in chamber and insertion into MRI RF probe. The soft cloth protects the fish and retains moisture. The chamber is then inserted into a 10 mm volume RF coil, with the fish's head positioned at the coil centre.

## 2.6 | MRI experiments

All scanning was performed on a 9.4 T MRI (Bruker BioSpec 70/30, Avance III spectrometer, 44 mm diameter vertical bore, 1,500 mT/m gradient strength, Bruker BioSpin MRI GmbH, Ettlingen, Germany). The probe was equipped with a 10 mm I.D.  $^1\text{H}/^{13}\text{C}$  dual channel volume coil. Each animal was placed vertically into the probe with its head up. The chamber was positioned so that the fish's head was located at the centre of a 10 mm  $^1\text{H}/^{13}\text{C}$  volume RF coil (M2M, Cleveland, OH, USA).

Scout images were acquired using FLASH (fast low angle shot; FOV 8 cm  $\times$  8 cm, matrix size 128  $\times$  128, flip angle 30°,  $TE/TR$  6/100 ms, three orthogonal slices, 2 mm slice thickness). To locate the brain more accurately two MSME (multi-slice multi-echo) spin echo scans were acquired in the axial and coronal planes (axial FOV 12 mm  $\times$  8 mm; matrix size 80  $\times$  60,  $TE/TR$  8.5/1500 ms, 17 slices, 500  $\mu\text{m}$  slice thickness; coronal FOV 12 mm  $\times$  8 mm; matrix size 128  $\times$  64,  $TE/TR$  14/1500 ms, 12 slices, 500  $\mu\text{m}$  slice thickness). Measurement of  $T_1$  and  $T_2$  was performed using a RARE-VTR sequence (rapid acquisition with refocused echoes-variable repetition time; FOV 12 mm  $\times$  5 mm, 100  $\mu\text{m}$   $\times$  100  $\mu\text{m}$  in plane resolution, 500  $\mu\text{m}$  slice thickness,  $TE$  10, 30, 50, 70 ms,  $TR$  1000, 1282, 1674, 2333, 5000 ms). Further high-resolution scans (50  $\mu\text{m}$   $\times$  50  $\mu\text{m}$  in plane resolution, 200 or 500  $\mu\text{m}$  slice thickness) were obtained with either MSME or RARE factor 2 scans, both  $TE/TR$  14/1500 ms. See figure legends for other details. The scan lasted for between 45 and 90 min.

## 2.7 | Data processing

Magnitude images were reconstructed without further modification using Bruker's ParaVision 5.1 software; these images were then imported into MATLAB (R2018b, MathWorks, Natick, MA, USA) for further analysis. Brain regions of interest (ROIs) were manually drawn by one of the authors (SR) for all image slices where brain tissue was observed. This region was further subdivided into fore, mid and hind regions; see Supporting Figure S9. Each ROI was drawn on images extracted from the shortest  $TE$ , longest  $TR$  of the RARE-VTR data set. Subsequently,  $T_1/T_2$  maps were calculated by fitting each voxel to the appropriate exponential equations ( $T_1$ ,  $M_0(1 - \exp[-t/T_1]) + c$ ;  $T_2$ ,  $M_0 \exp[-t/T_2] + c$ ) using the MATLAB 'Fit' function. Any fitted  $T_1$  values of more than 7000 ms,  $T_2$  values of more than 300 ms or fit function derived  $r^2$  values of less than 0.98 were rejected. Statistical analysis was performed on all of the voxels within an ROI by one-way ANOVA and Bonferroni post-hoc test (unless otherwise stated). Values are presented as mean  $\pm$  standard error of mean (SEM) unless otherwise stated.

Signal to noise ratios were determined from voxels within the brain ROI for each slice and a noise region within the slice (see FigShare for all images used and noise ROI regions). The images were the same as used for defining ROIs from the RARE-VTR images. The noise region consisted of two locations in the bottom left and right portions from the head end of the image containing a voxel square covering 10% of the image along short axis. The signal to noise ratio (SNR) was calculated as  $0.655 \times \text{mean (ROI voxel intensity)}/\text{standard deviation (combined noise ROI)}$ .<sup>17</sup>

## 3 | RESULTS

Using the life support chamber combined with the anaesthetic regime, we then tested the efficiency of the system to produce MRI scans clear of motion artefacts, such as water passage. Using MSME or RARE scans, images were obtained at 50  $\mu\text{m}$  in plane resolution and 0.2–0.5 mm slice thickness, requiring 30–90 min to acquire depending on slice thickness and number of averages (see Figure 3, and Figure S1 for gif videos showing images of the same fish live and fixed). Of the 29 fish that were scanned all were fully recovered, except for two scanned on the same day due to an overdose from tricaine. By calculating the SNR, we showed that images of live fish were comparable to those from fixed fish, with SNR higher in live fish compared with fixed fish, although this was not significant according to a paired Wilcoxon signed rank test; see Table 1 (individual fish images, including animal ages, are available on FigShare).

### 3.1 | Immersion in contrast agent refines common injection procedure for brain integrity analysis

To enhance SNR and reduce scanning time, we tested the addition of GCA using the common IP injection alongside a less invasive immersion approach. For each treatment group, heatmaps of  $T_1$  and  $T_2$  measurement were generated for each slice containing brain tissue (Figure 4). As expected, administration of GCA by injection caused a significant reduction in  $T_1$  voxel values of brain tissue compared with control fish groups (PBS injected and untreated; Figure 5A); mean  $T_1$  values (1590  $\pm$  27 ms) were significantly lower than for all other groups. The immersion method reduced  $T_1$  values (2341  $\pm$  20 ms) to significantly lower than for control groups: PBS injected (2955  $\pm$  20 ms) and untreated fish (3426  $\pm$  19 ms) (Figure 5A and Table S1 for  $p$  values). Two animals from the GCA immersion group had  $T_1$  values that were not significantly different from those of control fish, with one of them containing motion artefact (Figures S2 and S5; example images are available on FigShare). Nevertheless, immersion in GCA still provided an imaging advantage compared with the control groups and can be used to improve image quality instead of the more

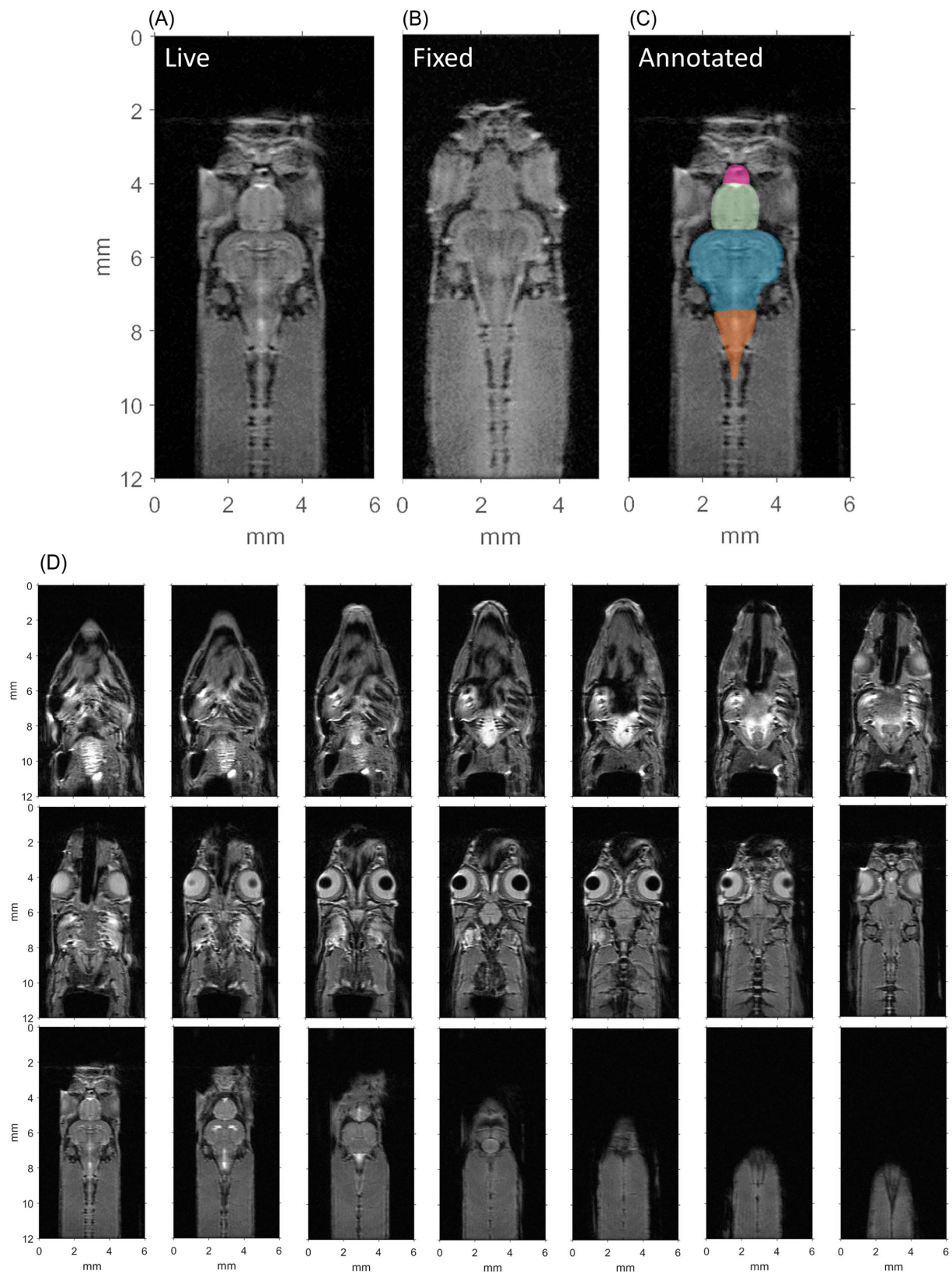


**FIGURE 3** (A, B), Spin echo images (RARE) from the same zebrafish live (A, FOV  $12\text{ mm} \times 6\text{ mm}$ ; scan time, 96 min) then fixed (B, FOV  $12\text{ mm} \times 5\text{ mm}$ ; scan time, 80 min). (C), Annotated anatomy showing olfactory bulbs (magenta), forebrain (green), midbrain (blue), hindbrain (orange). (D), Entire 4.2 mm stack of images from live fish. Imaging parameters:  $50\text{ }\mu\text{m} \times 50\text{ }\mu\text{m}$  in plane resolution,  $200\text{ }\mu\text{m}$  slice thickness,  $TE/TR$  14/1500 ms, number of excitations (NEX) 64. Animal age at scanning was 10 months old.

**TABLE 1** SNR for live and fixed fish within the brain ROI. Brain and noise ROI volumes are given in Table S7. Images for each animal, including brain and noise regions and volumes used, are available on [FigShare](#).

Treatment	N	SNR, mean (range)			$p^b$
		Live	Fixed	Ratio <sup>a</sup>	
GCA, injected	3	59 (55–67)	45 (37–50)	1.34	0.25
GCA, immersion	5	70 (47–84)	52 (40–60)	1.41	0.19
PBS, injected	3	65 (60–70)	47 (40–53)	1.40	0.25
Control	3	57 (51–63)	45 (41–51)	1.28	0.25

<sup>a</sup>SNR<sub>live</sub>/SNR<sub>fixed</sub> in the same animal (all brain ROI image slices), with the mean calculated per treatment.

<sup>b</sup>Wilcoxon signed rank test.

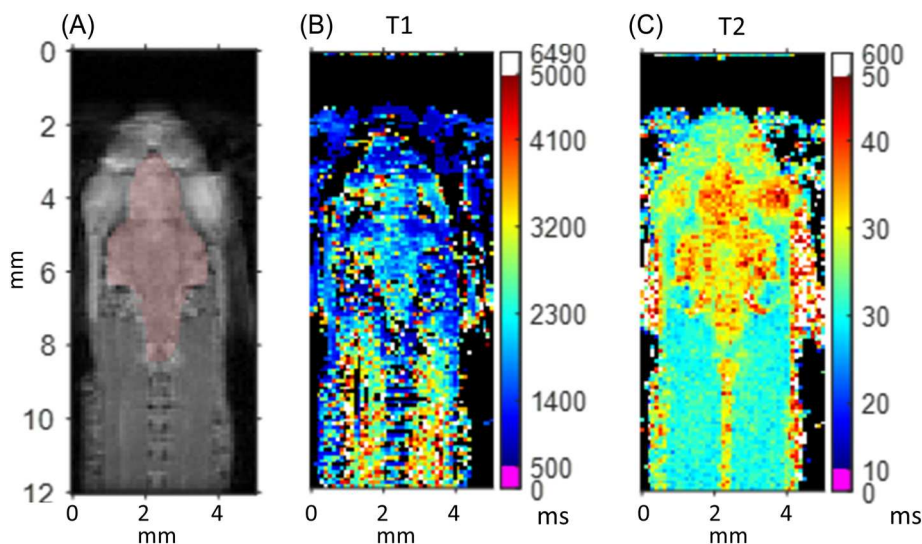


**FIGURE 4** Brain ROI used for  $T_1$  and  $T_2$  measurement. Example RARE-VTR showing ROI superimposed on magnitude image ( $TE$  10 ms,  $TR$  5000 ms) (A),  $T_1$  map (B) and  $T_2$  map (C). The colour bars to the right of the  $T_1$  and  $T_2$  maps depict the range of values. For clarity, the colour range was restricted such that values greater than 5000 ms ( $T_1$ ) or 50 ms ( $T_2$ ) are all set to white and values less than 500 ms ( $T_1$ ) or 10 ms ( $T_2$ ) are set to pink. Fish age at scanning was 10 months. Example images are available on [FigShare](#).

invasive IP injection (Figure 5A). ANOVA analysis was also performed using the mean  $T_1$  values for each brain ROI per animal. Similar trends were observed as above (see Supporting Figure S7).

As per  $T_1$  images, we observed significant changes in  $T_2$  voxel values in the GCA treated versus PBS/control fish (see Figure 5B and Supporting Table S2 for  $p$  values). Although IP injection of GCA showed the lowest  $T_2$  values ( $24.3 \pm 0.2$  ms), GCA immersion values ( $32.8 \pm 0.1$  ms) were still significantly lower than for control ( $34.4 \pm 0.1$  ms) and PBS injected ( $40.4 \pm 0.2$  ms) groups. Of note,  $T_2$  values for three of the GCA immersion fish were not significantly different from those of PBS injected/control fish; two of these were the same animals that also did not show significant change for the  $T_1$  data (Figures S4 and S6). ANOVA analysis was also performed using the mean  $T_2$  values for the brain ROI per animal. Similar trends were observed as above (see Supporting Figure S8).

To provide a comparison with fixed tissue MRI and assess GCA effects in this tissue, each animal scanned live was subsequently culled by immersion fixation in 4% PFA and scanned again 48 h after fixing. Overall, and irrespective of the treatment with GCA, the brain tissue of fixed fish showed  $T_1$  values that were significantly higher (ANOVA on all voxels) than in live fish for all groups except free swimming controls (Figure 5A and Table S3). Fixed fish  $T_1$  values for GCA treatment followed the same trend as for the live fish, with the exception that  $T_1$  values in PBS injected fish were not significantly different from those of control animals (Table S1). ANOVA analysis of the mean brain ROI  $T_1$  values for fixed animals showed similar trends, with GCA treated fish being significantly different from control fish.  $T_2$  values were very similar between all fixed groups, with significant differences (ANOVA of all voxels) only in  $T_2$  values for GCA treated groups (Tables S2 and S3). ANOVA analysis using the mean  $T_2$  values for the brain ROI per animal showed no significant differences between fixed fish.  $T_2$  values were significantly higher for the live brains compared with fixed samples (Figure 5B and Table S3).

We then asked whether  $T_1$  and  $T_2$  values could be extracted from different brain regions to provide a more detailed analysis. ROIs were manually drawn to separate the forebrain, the midbrain and the hindbrain regions (Figure S9). In live fish there were no significant differences in  $T_1$

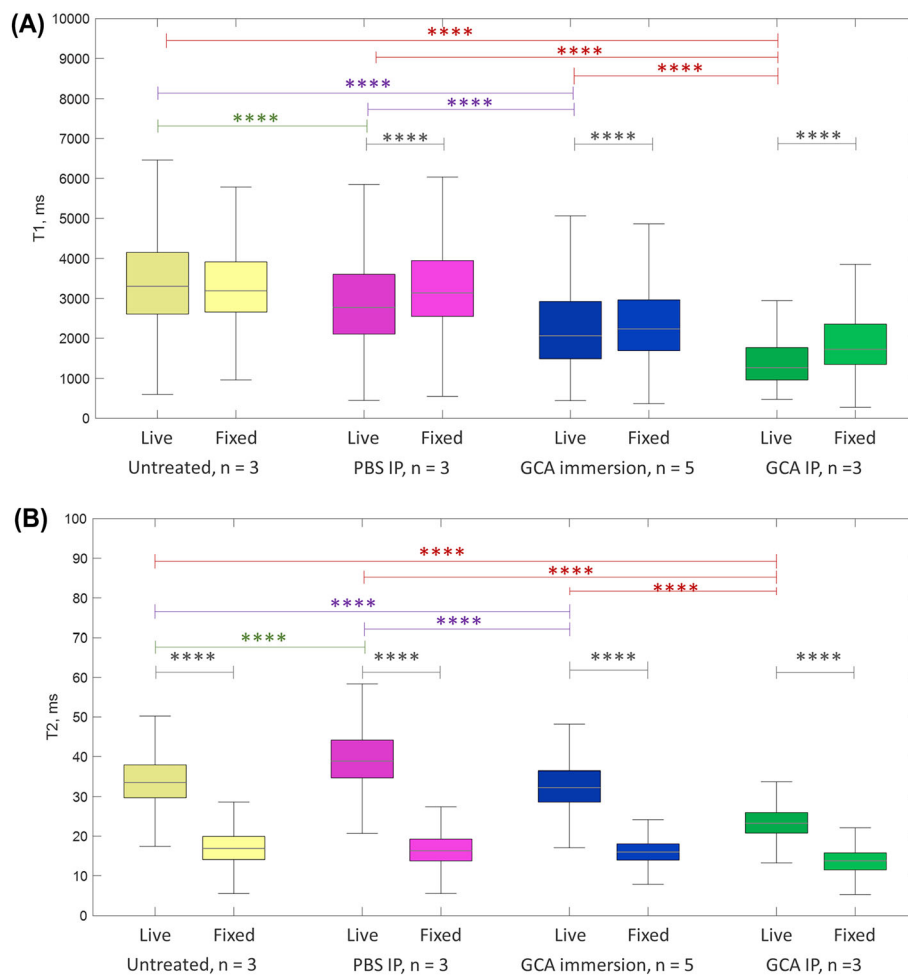


**FIGURE 5** GCA immersion improves image acquisition.  $T_1$  (A) and  $T_2$  (B) relaxation time measurements within the brain ROI of both live and fixed zebrafish. Prior to scanning, live fish were treated with GCA using IP injection or immersion or PBS using IP injection, or left untreated. The boxplots show the median and interquartile range (IQR), with the whisker located at  $1.5 \times$  IQR. Outliers have been removed for clarity and y-axis scaling (the full plot can be viewed in Supporting Figures S3 and S4, and outliers were included in the statistical analysis). The number of outliers represented 0.2–10.4% of the total number of voxels. Superimposed on the boxplots are the mean  $\pm$  SEM (crosses and error bars) from each animal brain ROI. Horizontal bars at the top of the plot show Bonferroni post hoc differences between live fish based on all of the voxels being tested. Statistical comparisons between the fixed fish groups are not shown. See Supporting Tables S1 and S2 for live and fixed fish details respectively. Example images are available on [FigShare](#). \*\*\*\* $p < 0.0001$ .

values between the ROIs (fore, mid or hind), irrespective of whether gadolinium had been administered or not (Figure S10a). However, after the fish had been fixed,  $T_1$  values were significantly different between brain ROIs for GCA immersion, PBS injected and control fish (Figure S10b and Table S4 for  $T_1$  and  $p$  values). In these three fixed fish cohorts, the forebrain ROI was significantly higher than the mid and hind ROIs. In contrast, there were no significant differences observed between brain ROIs for fixed fish injected with GCA.

In the case of brain ROI separated  $T_2$  values, significant differences in  $T_2$  values were observed for live fish; see Supporting Figure S11a. For each cohort,  $T_2$  values were highest in the forebrain region of GCA immersion, PBS injected and control fish, whilst the mid-brain ROI showed the highest  $T_2$  values for GCA injected fish (Table S5). A similar observation in the brain ROIs was made for fixed fish  $T_2$  values with significant differences between forebrain and midbrain ROIs in GCA injected, GCA immersion and PBS injected fish (as well as between fore and hind ROIs in the latter two cohorts). No significant differences were observed in the control group (Figure S11b and Table S6).

## 4 | DISCUSSION

Recently, a few bespoke chambers have been developed to sustain a live zebrafish during MRI scanning. These contain fully or partially water filled chambers,<sup>11–13</sup> whereas the chamber presented here used a more open design. This allowed the animal to be observed for well-being prior

to insertion into the magnet. Despite placing the fish in a vertical position for more than an hour there were no obvious signs of stress to the animal and the vast majority (27 out of 29) recovered within a few minutes when returned to freshwater. The open chamber design was also advantageous in that fish could be rapidly exchanged, and freely positioned vertically depending on their size. This versatility allowed the fish to be located such that the anatomical ROI could be placed at the most sensitive region of the RF coil. In principle, the fish could be moved sequentially in the vertical to image other anatomical regions. The chamber could easily be adapted to accept fish of varying sizes and could be redesigned for larger species that fitted within the volume of RF coils that were available to a facility.

We implemented an anaesthetic regime to minimize stress and allow full recovery of the animal after the scan. Tricaine is the most common anaesthetic used in zebrafish embryos as it immobilizes animals rapidly and efficiently for up to 48 h.<sup>16,18,19</sup> However, tricaine induces cardiac arrest in adult zebrafish after exposures as short as 15 min, therefore rendering its use limited for long term imaging and longitudinal studies.<sup>20,21</sup> A combination with either benzocaine or isoflurane was found to decrease risks of cardiac arrest and improve recovery.<sup>20,22,23</sup> Benzocaine is also known to allow longer staged anaesthesia.<sup>24</sup>

The imaging resolution obtained in this study was comparable to those previously described.<sup>12,13</sup> Generally, the image quality for live fish was similar to that of fixed fish, with a 30–40% improvement in SNR for live fish—most likely due to tissue fixative degrading the signal. The available signal to noise and imaging time ultimately limits the practical resolution and slice thickness that can be used, without excessively long anaesthetic times for the animal, due to signal averaging (example images are available on [FigShare](#)). On the other hand, fixed fish can be scanned for as long as one desires to achieve the required image resolution and SNR performance, but with the obvious lack of options for continuation of longitudinal studies or observing organ function. We limited our fish to less than 2 h of sedation. Improvements to RF coil design would help here, particularly if cry-cooled coils could be developed, or bespoke surface coils used. Alternatively, compressed sensing and systemic administration of GCAs could reduce scanning time due to  $T_1$  shortening, further reducing anaesthesia time.

$T_1$  values were higher in the control fish in this study (control live fish  $T_1$  3426 ± 19 ms) compared with those previously reported for freshly sacrificed fish ( $T_1$  1000–2000 ms;  $T_1$  2593 ± 138 ms, respectively).<sup>10,25</sup> The reason for the lower reported values in the Kline study could be due to their experiments being performed at 4 °C and 7 T. The temperature dependence of  $T_1$  has been shown in post-mortem human brain tissue, where  $T_1$  values can change by 3–17 ms/°C ( $T_2$  changes were more modest—0.2–0.3 ms/°C).<sup>26</sup> Additionally, the  $T_1$  values increase with magnetic field strength. Ullmann et al. estimated  $T_1$  values at a higher field strength (16.4 T) than ours.<sup>10</sup> However, they reported values from a single mid-sagittal slice (0.1 mm slice thickness) containing the telencephalon, hypothalamus and cerebellum, compared with our values for whole brain. Although  $T_1$  values were different, the  $T_2$  values in our study (control live fish  $T_2$  34.1 ± 0.1 ms) were comparable to those from the Kline et al. and Ullmann et al. studies (freshly sacrificed  $T_2$  30–50 ms and 22.13 ± 2.2 ms respectively). At low field clinically relevant magnetic field strengths,  $T_2$  relaxation remains largely constant. At ultrahigh field, more than 7 T, microscopic diffusion and magnetic susceptibility gradients can lead to a reduction in  $T_2$  values.<sup>27</sup>

The type of fixative applied to brain tissue has been reported to affect both  $T_1$  and  $T_2$  values in zebrafish.<sup>10</sup> Unlike Ullmann et al., we found a significant reduction in  $T_2$  values for fixed untreated fish compared with untreated live fish. This may have been due to the longer fixative immersion times used by us (>12 h) compared with Ullmann (3.5 h), and similar  $T_2$  reduction for longer fixation time was described by Thelwall et al., who applied fixative over a number of weeks.<sup>10,28</sup>  $T_2$  relaxation is sensitive to molecular motion and the addition of fixative changes the physical properties of the tissue, as well as potentially changing the exchange of protons between water molecules.<sup>10</sup> This influences  $T_2$  more than  $T_1$ —which is driven mainly by intramolecular dipolar relaxation between nuclei, well as with unpaired electrons present in a contrast agent. The significant variation in  $T_1$  and  $T_2$  values with brain region (fore, mid and hind) may be in part due to partial volume effects given the relatively large voxel size (100 μm) and slice thickness (500 μm). However, the similarity in  $T_1/T_2$  values between our and other studies should result in similar image contrast and quality for a given MRI imaging protocol.

GCAs have been used before in live zebrafish to shorten scanning time of the heart, but to our knowledge  $T_1$  and  $T_2$  values have only been reported in sacrificed fish. We investigated whether immersion of the fish in GCA doped tank water could be a viable alternative administration route to IP injection. Immersion administration of GCA offers an alternative to IP injection. The reductions in  $T_1$  and  $T_2$  values were between those of the IP administered GCA and the control cohorts (PBS, IP and control). However, in two of the five experiments there was no significant change in  $T_1$  or  $T_2$  values for the GCA immersion experiment. These experiments were performed similarly to the others, and it is unclear why the fish did not take up the GCA in sufficient quantities. Systemic biodistribution of GCA in adult zebrafish has been shown by Kline et al.<sup>25</sup> Absorption is probably similar between zebrafish and rodents, with Long et al. predicting bioavailability of drug-like molecules in zebrafish embryos.<sup>29</sup> Canaple et al. also showed GCA uptake and retention in early embryonic zebrafish development.<sup>30</sup> Adult zebrafish GCA excretion rates are unknown; however, they are likely to be similar to or faster than those for rodents (half-life: rat, 18–20 min; mouse, 5–6 min).<sup>31,32</sup> In our study, the GCA concentration and immersion time were not optimized. The immersion time was taken for pragmatic reasons whilst one of the other fish treatment groups was scanned. It is possible that similar changes in  $T_1/T_2$  could be achieved with shorter immersion times (<2 h), and these could be determined in future studies. However, GCA immersion should be considered where repeated IP injection could damage tissue, technical expertise in IP injection is not available or the small volume used could lead to IP dosing variation. Additionally, modifying the concentration of GCA could achieve a greater effect. However, it should be noted that the fish required a minimum of 100 mL tank water to swim in, and this necessitates the use of several millilitres of GCA for a specific concentration, whereas IP injection only requires a few microlitres.

## 5 | LIMITATIONS

The study used a relatively small number of animals in determining the effects of GCA administration. The number of animals used was decided on ethical considerations. Statistical analysis per animal is defined in the [ARRIVE guidelines for unit of assessment](#). To provide useful insight into the GCA methods used, our statistical analysis was performed both per animal and per voxel, with both showing similar significant differences between groups. It was assumed that GCA immersion fish had attained steady state gadolinium uptake by the time of scanning. Signal to noise and imaging time are always a trade-off in MRI. For zebrafish imaging, voxel resolution must high to avoid partial volume effects, demanding long imaging time and ultra-high field scanners.

## 6 | CONCLUSIONS AND PERSPECTIVES

Animal research and the NC3Rs have steadily transitioned towards studying disease in zebrafish. This has focused on embryonic/juvenile animals due to their amenability to optical imaging. There is increasing interest in the diseases of old age, coupled with healthy aging. Here, we describe the first vertical life support chamber and its use for MRI scanning of adult zebrafish, which we used to refine current injection protocol of contrast agent by using non-invasive immersion instead. Fish between 10 and 18 months were scanned and all but two fish were fully recovered, indicating the chamber's potential in longitudinal studies. There are no technical obstacles to extending the fish age range to younger and older animals. The results showed that immersing the fish in gadolinium doped water is a viable alternative to injection, which may be advantageous in a small animal where the injection site is difficult to access.

By providing longitudinal analysis of zebrafish brain tissue in later life, MRI will help to widen the use of zebrafish in modelling neurodegenerative diseases and their progression. The versatility of MRI goes beyond that of simple structural images. The ability to measure other physiologically relevant parameters such as diffusion, perfusion and blood flow could aid the study of disease progression.<sup>33</sup> Improvements to RF coil sensitivity could also allow single voxel spectroscopy to identify brain metabolites. Zebrafish MRI could offer a cheap and accessible route to the study of other organs such as the heart.

### ACKNOWLEDGEMENTS

This work has been supported by a European Leukodystrophy Association fellowship (ELA 2016-012F4, Association Européenne contre les Leucodystrophies) to NH and a University of Sheffield Alumni Fund: Flagship Institute Research Award to NH and SR. We are grateful to Dr Alan Hart, our Director of Biological Services, for his continued support to help us navigate through zebrafish Home Office regulations and make this project a success.

### AUTHOR CONTRIBUTIONS

NH and SR acquired funding, designed the study, collected and analysed data and wrote the manuscript. CA designed the study, advised on Home Office regulations and revised the manuscript.

### CONFLICTS OF INTEREST

The authors declare that the research was conducted in the absence of any commercial or financial relationship that could be construed as a potential conflict of interest.

### ORCID

Noémie Hamilton  <https://orcid.org/0000-0002-3299-9133>

Steven Reynolds  <https://orcid.org/0000-0002-6463-8471>

### REFERENCES

1. Burrows DJ, McGown A, Jain SA, et al. Animal models of multiple sclerosis: from rodents to zebrafish. *Mult Scler*. 2019;25(3):306-324. doi:[10.1177/1352458518805246](https://doi.org/10.1177/1352458518805246)
2. Hamilton N, Rutherford HA, Petts JJ, et al. The failure of microglia to digest developmental apoptotic cells contributes to the pathology of RNASET2-deficient leukoencephalopathy. *Glia*. 2020;68(7):1531-1545. doi:[10.1002/glia.23829](https://doi.org/10.1002/glia.23829)
3. Keatinge M, Bui H, Menke A, et al. Glucocerebrosidase 1 deficient *Danio rerio* mirror key pathological aspects of human Gaucher disease and provide evidence of early microglial activation preceding alpha-synuclein-independent neuronal cell death. *Hum Mol Genet*. 2015;24(23):6640-6652. doi:[10.1093/hmg/ddv369](https://doi.org/10.1093/hmg/ddv369)
4. Najib NHM, Nies YH, Abd Halim SAS, et al. Modeling Parkinson's disease in zebrafish. *CNS Neurol Disord Drug Targets*. 2020;19(5):386-399. doi:[10.2174/1871527319666200708124117](https://doi.org/10.2174/1871527319666200708124117)
5. Rutherford HA, Hamilton N. Animal models of leukodystrophy: a new perspective for the development of therapies. *FEBS J*. 2019;286(21):4176-4191. doi:[10.1111/febs.15060](https://doi.org/10.1111/febs.15060)

6. Yakshi E, Jamali A, Diaz Verdugo C, Jurisch-Yakshi N. Past, present and future of zebrafish in epilepsy research. *FEBS J*. 2021;288(24):7243-7255. doi:10.1111/febs.15694
7. Denic A, Macura SI, Mishra P, Gamez JD, Rodriguez M, Pirko I. MRI in rodent models of brain disorders. *Neurotherapeutics*. 2011;8(1):3-18. doi:10.1007/s13311-010-0002-4
8. Dijkhuizen RM, Nicolay K. Magnetic resonance imaging in experimental models of brain disorders. *J Cereb Blood Flow Metab*. 2003;23(12):1383-1402. doi:10.1097/01.WCB.0000100341.78607.EB
9. Haud N, Kara F, Diekmann S, et al. rnas2 mutant zebrafish model familial cystic leukoencephalopathy and reveal a role for RNase T2 in degrading ribosomal RNA. *Proc Natl Acad Sci U S A*. 2011;108(3):1099-1103. doi:10.1073/pnas.1009811107
10. Ullmann JF, Cowin G, Kurniawan ND, Collin SP. Magnetic resonance histology of the adult zebrafish brain: optimization of fixation and gadolinium contrast enhancement. *NMR Biomed*. 2010;23(4):341-346.
11. Kabli S, Spaink HP, De Groot HJ, Alia A. In vivo metabolite profile of adult zebrafish brain obtained by high-resolution localized magnetic resonance spectroscopy. *J Magn Reson Imaging*. 2009;29(2):275-281. doi:10.1002/jmri.21609
12. Koth J, Maguire ML, McClymont D, et al. High-resolution magnetic resonance imaging of the regenerating adult zebrafish heart. *Sci Rep*. 2017;7(1):2917. doi:10.1038/s41598-017-03050-y
13. Merrifield GD, Mullin J, Gallagher L, et al. Rapid and recoverable in vivo magnetic resonance imaging of the adult zebrafish at 7T. *Magn Reson Imaging*. 2017;37:9-15. doi:10.1016/j.mri.2016.10.013
14. Wahsner J, Gale EM, Rodriguez-Rodriguez A, Caravan P. Chemistry of MRI contrast agents: current challenges and new frontiers. *Chem Rev*. 2019;119(2):957-1057. doi:10.1021/acs.chemrev.8b00363
15. Nüsslein-Volhard C, Dahm R. *Zebrafish: a Practical Approach*. Oxford University Press; 2002.
16. Westerfield M. *The Zebrafish Book: a Guide for the Laboratory Use of Zebrafish (Danio rerio)*. University of Oregon Press; 1995.
17. Firbank MJ, Coulthard A, Harrison RM, Williams ED. A comparison of two methods for measuring the signal to noise ratio on MR images. *Phys Med Biol*. 1999;44(12):N261-N264. doi:10.1088/0031-9155/44/12/403
18. Kaufmann A, Mickoleit M, Weber M, Huysen J. Multilayer mounting enables long-term imaging of zebrafish development in a light sheet microscope. *Development*. 2012;139(17):3242-3247. doi:10.1242/dev.082586
19. Kimmel CB, Ballard WW, Kimmel SR, Ullmann B, Schilling TF. Stages of embryonic development of the zebrafish. *Dev Dyn*. 1995;203(3):253-310. doi:10.1002/aja.1002030302
20. Huang WC, Hsieh YS, Chen IH, et al. Combined use of MS-222 (tricaine) and isoflurane extends anesthesia time and minimizes cardiac rhythm side effects in adult zebrafish. *Zebrafish*. 2010;7(3):297-304. doi:10.1089/zeb.2010.0653
21. Matthews M, Varga ZM. Anesthesia and euthanasia in zebrafish. *ILAR J*. 2012;53(2):192-204. doi:10.1093/ilar.53.2.192
22. Lockwood N, Parker J, Wilson C, Frankel P. Optimal anesthetic regime for motionless three-dimensional image acquisition during longitudinal studies of adult nonpigmented zebrafish. *Zebrafish*. 2017;14(2):133-139.
23. Wynd BM, Watson CJ, Patil K, Sanders GE, Kwon RY. A dynamic anesthesia system for long-term imaging in adult zebrafish. *Zebrafish*. 2017;14(1):1-7.
24. Olt J, Allen CE, Marcotti W. In vivo physiological recording from the lateral line of juvenile zebrafish. *J Physiol*. 2016;594(19):5427-5438. doi:10.1113/JP271794
25. Kline TL, Sussman CR, Irazabal MV, et al. Three-dimensional NMR microscopy of zebrafish specimens. *NMR Biomed*. 2019;32(1):e4031. doi:10.1002/nbm.4031
26. Birkl C, Langkammer C, Golob-Schwarzl N, et al. Effects of formalin fixation and temperature on MR relaxation times in the human brain. *NMR Biomed*. 2016;29(4):458-465. doi:10.1002/nbm.3477
27. de Graaf RA, Brown PB, McIntyre S, Nixon TW, Behar KL, Rothman DL. High magnetic field water and metabolite proton  $T_1$  and  $T_2$  relaxation in rat brain in vivo. *Magn Reson Med*. 2006;56(2):386-394. doi:10.1002/mrm.20946
28. Thelwall PE, Shepherd TM, Stanisiz GJ, Blackband SJ. Effects of temperature and aldehyde fixation on tissue water diffusion properties, studied in an erythrocyte ghost tissue model. *Magn Reson Med*. 2006;56(2):282-289. doi:10.1002/mrm.20962
29. Long K, Kostman SJ, Fernandez C, Burnett JC, Hury DM. Do zebrafish obey Lipinski rules? *ACS Med Chem Lett*. 2019;10(6):1002-1006. doi:10.1021/acsmchemlett.9b00063
30. Canaple L, Beuf O, Armenean M, Hasserodt J, Samarut J, Janier M. Fast screening of paramagnetic molecules in zebrafish embryos by MRI. *NMR Biomed*. 2008;21(2):129-137. doi:10.1002/nbm.1169
31. Aime S, Caravan P. Biodistribution of gadolinium-based contrast agents, including gadolinium deposition. *J Magn Reson Imaging*. 2009;30(6):1259-1267. doi:10.1002/jmri.21969
32. Davies J, Siebenhandl-Wolff P, Tranquart F, Jones P, Evans P. Gadolinium: pharmacokinetics and toxicity in humans and laboratory animals following contrast agent administration. *Arch Toxicol*. 2022;96(2):403-429. doi:10.1007/s00204-021-03189-8
33. Patton EE, Zon LI, Langenau DM. Zebrafish disease models in drug discovery: from preclinical modelling to clinical trials. *Nat Rev Drug Discov*. 2021;20(8):611-628. doi:10.1038/s41573-021-00210-8

## SUPPORTING INFORMATION

Additional supporting information can be found online in the Supporting Information section at the end of this article.

**How to cite this article:** Hamilton N, Allen C, Reynolds S. Longitudinal MRI brain studies in live adult zebrafish. *NMR in Biomedicine*. 2023; e4891. doi:10.1002/nbm.4891